Inorg. Chem. **2008**, *47*, 7286−7294

How Close Can You Get? Studies of Ultrafast Light-Induced Processes in Ruthenium-[60] Fullerene Dyads with Short Pyrazolino and Pyrrolidino Links

Susanne Karlsson,[‡] Judit Modin,[†] Hans-Christian Becker,[‡] Leif Hammarström,[‡] and Helena Grennberg*[,†]

Department of Biochemistry and Organic Chemistry, Uppsala University, Box 576, SE- 751 24 Uppsala, Sweden, and Department of Photochemistry and Molecular Science, Chemical Physics, Uppsala University, Box 523, SE-751 20 Uppsala, Sweden

Received January 28, 2008

Two pyrazoline- and one pyrrolidine-bridged Ru(II)bipyridine-[60]fullerene dyads have been prepared and studied by ultrafast time-resolved spectroscopy. A silver-assisted synthesis route, in which Ag(I) removes the chlorides from the precursor complex $Ru(bpy)_2Cl_2$ facilitates successful coordination of the [60]fullerene-substituted third ligand. Upon light excitation of the ruthenium moiety, the emission was strongly quenched by the fullerene. The main quenching mechanism is an exceptionally fast direct energy transfer ($k_{obs} > 1 \times 10^{12}$ s^{-1} in the pyrazoline-bridged dyads), resulting in population of the lowest excited triplet state of fullerene. No evidence for electron transfer was found, despite the extraordinarily short donor−acceptor distance that could kinetically favor that process. The observations have implications on the ongoing development of devices built from Ru-polypyridyl complexes and nanostructured carbon, such as C_{60} or nanotubes.

Introduction

Octahedral complexes of ruthenium(II) with bipyridine type ligands are frequently used in donor−acceptor assemblies. They are suitable sensitizers due to their photostability and high ^{3}MLCT excited-state energy, combined with favorable electron acceptor and donor properties.[1,2] For example, $Ru(bpy)_3$ and similar motifs are used in studies toward artificial photosynthesis[2−7] and in TiO_2-based dye-sensitized solar cells.[8,9] With catalysis of many-electron processes being one of the major challenges in current photochemistry, studies of systems where Ru(II) is combined with acceptor units capable of accepting several electrons are of great importance.

The [60]fullerene has the ability to accumulate up to six electrons in successive reductions within a 2 V potential range.[10,11] Its small reorganization energy and favorable acceptor properties have in recent years attracted interest, and many fullerene donor−acceptor dyads and triads have been produced.[12−15] Also, [60]fullerene can serve as a molecular model for functionalization and sensitization of

* To whom correspondence should be addressed. E-mail: Helena.Grennberg@biorg.uu.se.
‡ Department of Photochemistry and Molecular Science.
† Department of Biochemistry and Organic Chemistry.

(1) Juris, A.; Balzani, V.; Barigelletti, F.; Campagna, S.; Belser, P.; Zelewsky, A. V. *Coord. Chem. Rev.* **1988**, *84*, 85–277.
(2) *Covalently Linked Systems Containing Metal Complexes*; Scandola, F.; Chiorboli, C.; Indelli, M. T.; Rampi, M. A., Eds.; Wiley-VCH: New York, 2001; Vol. *3*.
(3) Alstrum-Acevedo, J. H.; Brennaman, M. K.; Meyer, T. J. *Inorg. Chem.* **2005**, *44*, 6802–6827.
(4) Burdinski, D.; Wieghardt, K.; Steenken, S. *J. Am. Chem. Soc.* **1999**, *121*, 10781–10787.
(5) Falkenström, M.; Johansson, O.; Hammarström, L. *Inorg. Chim. Acta* **2007**, *360*, 741–750.
(6) Sun, L.; Hammarström, L.; Åkermark, B.; Styring, S. *Chem. Soc. Rev.* **2001**, *30*, 36–49.
(7) Baranoff, E.; Collin, J. P.; Flamigni, L.; Sauvage, J. P. *Chem. Soc. Rev.* **2004**, *33*, 147–155.
(8) Hagfeldt, A.; Grätzel, M. *Acc. Chem. Res.* **2000**, *33*, 269–277.
(9) Meyer, G. J. *Inorg. Chem.* **2005**, *44*, 6852–6864.
(10) Xie, Q.; Pérez-Cordero, E.; Echegoyen, L. *J. Am. Chem. Soc.* **1992**, *114*, 3978–3980.
(11) Echegoyen, L.; Echegoyen, L. E. *Acc. Chem. Res.* **1998**, *31*, 593–601.
(12) Guldi, D.; Prato, M. *Acc. Chem. Res.* **2000**, *33*, 695–703.
(13) Martín, N.; Sánchez, L.; Illescas, B.; Pérez, I. *Chem. Rev.* **1998**, *98*, 2527–2547.
(14) Meijer, M. D.; van Klink, G. P. M.; van Koten, G. *Coord. Chem. Rev.* **2002**, *230*, 141–163.
(15) Diekers, M.; Hirsch, A.; Pyo, S.; Rivera, J.; Echegoyen, L. *Eur. J. Org. Chem.* **1998**, *1998*, 1111–1121.

10.1021/ic800168d CCC: $40.75
Published on Web 07/18/2008

Chart 1. Structures of the Ru(II) Complexes **1**−**6**

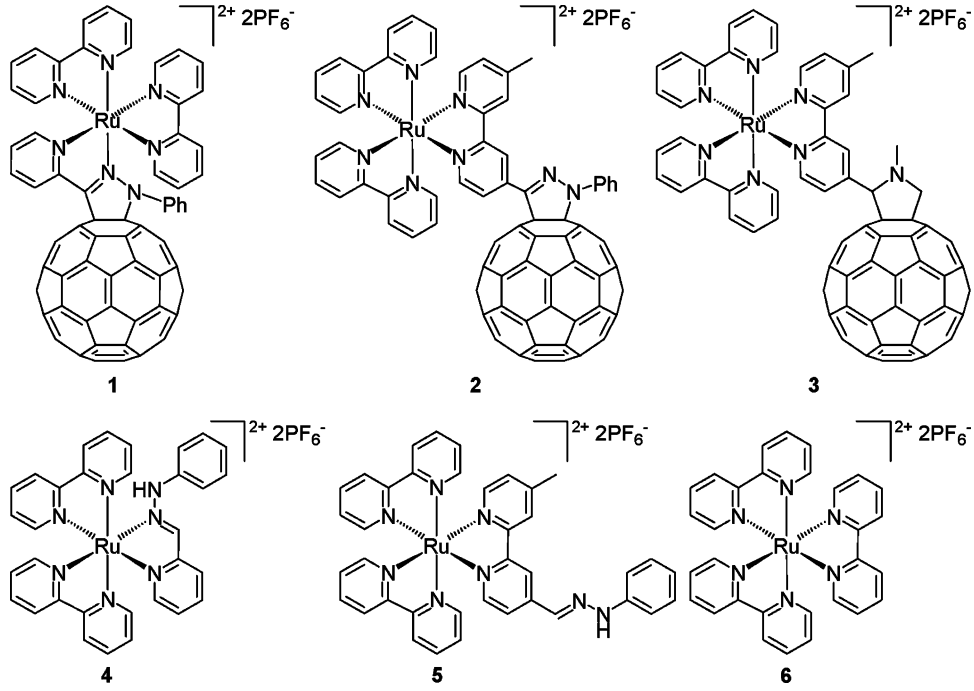

carbon nanotubes using near-identical chemical transformations,[16] an important topic in current nanomaterials science.

Previous studies of the $Ru(bpy)_3$-C_{60} pair have, with a few exceptions,[17–20] shown that charge separation is often outcompeted by energy transfer, typically on the nanosecond time scale ($k_{obs} = 5 \times 10^7$ to 1.5×10^9 s^{-1}).[21–26] If the rate of electron transfer can be increased by dyad design, it may however favorably compete with direct energy transfer, leading to a population of the charge-separated state. As most $Ru(bpy)_3$-C_{60} dyads produced to date have long links, we were interested in studying the effect of very short linking motifs.

The rates of nonadiabatic electron transfer and exchange energy transfer are expected to increase as the donor−acceptor distance decreases.[27,28] The electronic coupling, V_{DA}, will be the major contribution to this, as it decreases exponentially with the donor−acceptor distance, in which electron transfer and exchange energy transfer show a very similar distance dependence.[29,30] In addition, the rate of electron transfer (but notably not that of energy transfer) is expected to increase due to a decrease in reorganization energy λ, which is strongly dependent on the donor−acceptor distance. Also, the driving force for electron transfer will increase due to stabilization of the charge-separated state by Coulombic interaction. The effective rates of energy and electron transfer are thus dependent on the electronic coupling in the dyad, driving force for the reaction, and the reorganization energy. The a priori evaluation of these factors is not trivial. Everything else being equal, a short link between donor and acceptor may in principle favor electron transfer more than exchange energy transfer, mainly due to the effect of decreased reorganization energy.

In the present article, we discuss alternative synthetic routes and photophysical properties of three [60]fullerene-containing ruthenium-LL′ dyad complexes.[31] In dyads **1** and **2** (Chart 1), the donor and acceptor are connected via a pyrazoline bridge, whereas the third complex, **3**, contains a pyrrolidine bridge. We also present the preparation and initial photophysical characterization of two new $Ru(II)(bpy)_2(LL')$ complexes **4** and **5** that are related to **1** and **2**, respectively.

(16) Grennberg, H.; Li, J. *Chem.*−*Eur. J.* **2006**, *12*, 3869–3875.
(17) Sariciftci, N.; Wudl, F.; Heeger, A.; Maggini, M.; Scorrano, G.; Prato, M.; Bourassa, J.; Ford, P. *Chem. Phys. Lett.* **1995**, *247*, 510–514.
(18) Polese, A.; Mondini, S.; Bianco, A.; Toniolo, C.; Scorrano, G.; Guldi, D.; Maggini, M. *J. Am. Chem. Soc.* **1999**, *121*, 3446–3452.
(19) Armaroli, N.; Accorsi, G.; Felder, D.; Nierengarten, J.-F. *Chem.*−*Eur. J.* **2002**, *8*, 2314–2323.
(20) Maggini, M.; Guldi, D.; Mondini, S.; Scorrano, G.; Paolucci, F.; Ceroni, P.; Roffia, S. *Chem.*−*Eur. J.* **1998**, *4*, 1992–2000.
(21) Guldi, D.; Maggini, M.; Menna, E.; Scorrano, G.; Ceroni, P.; Marcaccio, M.; Paolucci, F.; Roffia, S. *Chem.*−*Eur. J.* **2001**, *7*, 1597–1605.
(22) Allen, B.; Benniston, A.; Harriman, A.; Mallon, L.; Pariani, C. *Phys. Chem. Chem. Phys.* **2006**, *8*, 4112–4118.
(23) Chaignon, F.; Torroba, J.; Blart, E.; Borgström, M.; Hammarström, L.; Odobel, F. *New J. Chem.* **2005**, *29*, 1272–1284.
(24) Zhou, Z.; Sarova, G.; Zhang, S.; Ou, Z.; Tat, F.; Kadish, K.; Echegoyen, L.; Guldi, D.; Schuster, D.; Wilson, S. *Chem.*−*Eur. J.* **2006**, *12*, 4241–4248.
(25) McNally, A.; Forster, R. J.; Russel, N. R.; Keyes, T. E. *Dalton Trans.* **2006**, *2006*, 1729–1737.
(26) Possamai, G.; Menna, E.; Maggini, M.; Carano, M.; Marcaccio, M.; Paolucci, F.; Guldi, D. M.; Swartz, A. *Photochem. Photobiol. Science* **2006**, *5*, 1154–1164.
(27) Marcus, R. A.; Sutin, N. *Biochim. Biophys. Acta* **1985**, *811*, 265–322.
(28) Dexter, D. L. *J. Chem. Phys.* **1953**, *21*, 836–850.
(29) Closs, G. L.; Piotrowiak, P.; MacInnis, J. M.; Fleming, G. R. *J. Am. Chem. Soc.* **1988**, *110*, 2652–2653.
(30) Closs, G. L.; Johnson, M. D.; Miller, J. R.; Piotrowiak, P. *J. Am. Chem. Soc.* **1989**, *111*, 3751–3753.
(31) Modin, J.; Johansson, H.; Grennberg, H. *Org. Lett.* **2005**, *7*, 3977–3979.

The links in **1**−**3** are very short, minimizing the donor−acceptor distance, which will affect the rates of both energy and electron transfer as discussed above. There are several examples in the literature of ruthenium-[60]fullerenes with the pyrrolidine functionalization, but the pyrazoline has to our knowledge not yet been studied in $Ru(bpy)_3$-C_{60} dyads. To our knowledge there is only one previous study on a dyad with a donor−acceptor through-bond distance similar to that of **3**. That dyad, as is the case for **3**, has a pyrrolidine linking motif and did not undergo electron transfer.[24] With the pyrazoline functionalization (especially in **1**), the donor−acceptor distance is even shorter. The conjugated pyrazoline functionalization is expected to increase the electronic coupling compared to the pyrrolidine, thus in particular dyads **1** and **2** are interesting for studies of fundamental photophysical properties.

Experimental Section

All reagents, including $Ru(bpy)_3(PF_6)_2$ **6**, were obtained from commercial sources and were used without further purification except for the toluene that was distilled from sodium prior to use. The preparation of bis(2,2′-bipyridine)(1′,5′-dihydro-3′-methyl-2′-(4-(4′-methyl-2,2′-bipyridinyl)-2′H-[5,6]fullereno(C_{60}-I_h)[1,9]pyrrole)ruthenium-bis(hexafluorophosphate) **3** by complexation to $Ru(bpy)_2Cl_2 \cdot 2H_2O$, and ligands **7**−**11** has been described elsewhere.[31] Column chromatography was performed using Matrex Silica 60A/35−70 μm as a solid phase. Thin layer chromatography (TLC) was performed on Merck precoated silica gel 60-F_{254} plates. ^{1}H NMR spectra were recorded on a Varian Inova 500 spectrometer (499.9 MHz) and ^{13}C NMR spectra on a Varian Unity 400 spectrometer (100.6 MHz). The chemical shifts are reported using the residual solvent signal as an indirect reference to TMS: acetone-d_6 2.05 ppm (^{1}H).

Photophysical measurements were performed in spectroscopic grade acetonitrile or CH_2Cl_2 at 298 K. Absorption spectra were recorded for acetonitrile solutions on an HP 8453 diode array instrument. The approximate optical density of the samples was 0.1−0.2 at 450 nm (0.3 for single wavelength pump−probe spectroscopy).

Bis(2,2′-bipyridine)(2′-phenyl-5′-(2-pyridinyl)-2′H-[5,6]fullereno(C_{60}-I_h)[1,9]pyrazole)ruthenium-bis(hexafluorophosphate) (1). To a solution of 2′-phenyl-5′-(2-pyridinyl)-2′H-[5,6]fullereno(C_{60}-I_h)[1,9]pyrazole (25 mg, 27 μmol) **7** in toluene (10 mL) kept under inert atmosphere, $Ru(bpy)_2Cl_2 \cdot 2H_2O$ (14 mg, 27 μmol), $AgBF_4$ (10 mg 51 μmol) and 2-methoxyethanol (10 mL) were added. The mixture was heated to 130 °C for 12 h, and the brown-red suspension was cooled to ambient temperature. After the addition of NH_4PF_6 (89 mg, 545 μmol) dissolved in water (1 mL), the solvents were removed. The residue was partially dissolved in water and filtered. The solid remains after the filtration was dissolved in a small amount of acetone, and diethyl ether was added until a precipitation occurred. Filtration, washing with diethyl ether, and drying the solid in vacuo yielded 17 mg **1** (32%). ESI-MS was in accordance with literature.[31] ^{1}H NMR (aceton-d_6) δ = 6.94 (1H), 6.95 (1H), 7.13 (1H), 7.17−7.22 (2H), 7.34 (1H), 7.54 (1H), 7.57 (1H), 7.64 (2H), 7.77 (1H), 7.85 (1H), 7.90−7.96 (3H), 8.02 (1H), 8.20 (1H), 8.24−8.28 (3H), 8.34−8.38 (2H), 8.39 (1H), 8.47 (1H), 8.52 (1H), 8.62 (1H), 8.74 (1H), 8.83 (1H), 8.86 (2H), 9.24 (1H), 8.30 (1H), 9.72 (1H). The five extra proton signals might originate from isomers due to unusually slow pyramidal inversion of the tertiary amine.

Bis(2,2′-bipyridine)(2′-Phenyl-5′-(4-(4′-methyl-2,2′-bipyridinyl)-2′H-[5,6]fullereno(C_{60}-I_h)[1,9]pyrazole)ruthenium-bis(hexafluorophosphate) (2). A round-bottomed flask containing 2′-phenyl-5′-(4-(4′-methyl-2,2′-bipyridinyl)-2′H-[5,6]fullereno(C_{60}-I_h)[1,9]pyrazole **8** (25 mg, 27 μmol), $Ru(bpy)_2Cl_2 \cdot 2H_2O$ (13.9 mg, 27 μmol), and $AgBF_4$ (13 mg, 67 μmol) was put on the vacuum line for 2 h before ethanol (4 mL) and toluene (4 mL) was added, and the mixture was heated to 100 °C for 20 h and cooled to ambient temperature. The remaining solids were filtered off and washed with ethanol (1 mL). To the solution was added NH_4PF_6 (87 mg, 535 μmol) as a solid. The resulting precipitate was removed by filtration and washed with water, and ether and then dried in vacuo to give **2** in 35% yield. From the solution, 10 mg of starting material mixture was recovered by extraction with CH_2Cl_2. ESI-MS of **2** was in accordance with the literature.[31] ^{1}H NMR (aceton-d_6) δ = 2.60 (3H), 7.42−7.48 (2H), 7.52−7.62 (6H), 7.91 (1H), 8.02−8.08 (4H), 8.11−8.25 (7H), 8.58 (1H), 8.76−8.85 (5H), 9.67 (1H).

Bis(2,2′-bipyridine)(2-((2-phenylhydrazono)methyl)pyridine)-ruthenium- bis(hexafluorophosphate) (4). To 2-((2-phenylhydrazono)methyl)pyridine **10** (4.9 mg, 25 μmol) and $Ru(bpy)_2Cl_2 \cdot 2H_2O$ (13 mg, 25 μmol) under an inert atmosphere was added ethanol (5 mL) and the solution was refluxed for 4 h. To the cooled solution was added NH_4PF_6 (81 mg, 500 μmol) as a solution in 3 mL water. Most of the solvent was evaporated until precipitation occurred. The solids were then removed by filtration, washed with water and ether, and then dried in vacuo to give **4** in 62% yield.[1] ^{1}H NMR (acetone-d_6) δ = 6.88 (1H, m), 7.25 (3H, m), 7.39 (1H, ddd, J = 1.5, 5.7, 7.6 Hz), 7.43 (1H, ddd, J = 1.3, 5.7, 7.6 Hz), 7.57 (1H, ddd, J = 1.3, 5.6, 7.6 Hz), 7.76 (1H, ddd, J = 1.4, 5.6, 7.7 Hz), 7.85 (1H, ddd, J = 1.3, 5.6, 7.7 Hz), 7.86 (1H, ddd, J = 0.8, 1.4, 5.7 Hz), 7.96 (1H, ddd, J = 0.8, 1.5, 5.6 Hz), 7.99 (1H, ddd, J = 0.8, 1.5, 4.8 Hz), 8.00 (1H, ddd, J = 0.8, 1.5, 4.9 Hz), 8.03 (1H, ddd, J = 1.4, 7.6, 8.0 Hz), 8.04 (1H, ddd, J = 1.5, 7.7, 8.1 Hz), 8.14 (1H, ddd, J = 0.8, 1.5, 8.0 Hz), 8.21 (1H, ddd, J = 1.5, 7.6, 8.1 Hz), 8.29 (1H, ddd, J = 1.5, 7.7, 8.2 Hz), 8.35 (1H, ddd, J = 1.5, 7.6, 8.2 Hz), 8.59 (1H, ddd, J = 0.8, 1.3, 8.4 Hz), 8.61 (1H, m), 8.78 (1H, ddd, J = 0.8, 1.4, 8.2 Hz), 7.79 (1H, ddd, J = 0.8, 1.3, 8.2 Hz), 8.82 (1H, ddd, J = 0.8, 1.3, 8.2 Hz), 8.96 (1H, ddd, J = 0.8, 1.5, 5.6 Hz), 9.06 (1H, br s).

Bis(2,2′-bipyridine) 4-methyl-4′-((2-phenylhydrazono)methyl)-2,2′-bipyridine)ruthenium-bis(hexafluorophosphate) (5). To 4-methyl-4′-((2-phenylhydrazono)methyl)-2,2′-bipyridine (15 mg, 52 μmol) **11** and $Ru(bpy)_2Cl_2 \cdot 2H_2O$ (27 mg, 52 μmol) under an inert atmosphere was added ethanol (5 mL) and the solution was refluxed for 15 h. To the cooled solution was added NH_4PF_6 (170 mg, 1.04 mmol) and water (2 mL) to form a precipitate. The solids were removed by filtration, washed with water and ether, and dried in vacuo to give **5** in 68% yield. ^{1}H NMR (aceton-d_6) δ = 2.64 (3H), 6.92 (1H), 7.01 (1H), 7.23 (1H), 7.28 (1H), 7.35 (2H), 7.42 (1H), 7.55−7.62 (3H), 7.74 (1H), 7.76 (1H), 7.85 (1H), 7.97 (1H), 8.06 (1H), 8.07 (1H), 8.10 (1H), 8.17 (1H), 8.18−8.23 (4H), 8.60 (1H), 8.74 (1H), 8.80−8.84 (3H), 8.87 (2H).

Electrochemistry. Cyclic voltammetry and differential pulse voltammetry were carried out using a small volume (200 μL) three-electrode setup in a Faraday cage, connected to an Autolab potentiostat with a GPES electrochemical interface (Eco Chemie). Solutions were prepared from spectroscopic grade acetonitrile with 0.1 M tetrabutylammonium hexafluorophosphate ($TBAPF_6$) as supporting electrolyte and an approximate analyte concentration of 2 mM. Analytes were added as PF_6 salts. Oxygen was removed in all measurements by argon purging, and the measurements where conducted under argon atmosphere. The working electrode was a

Scheme 1. The Two Major Routes to Dyads Consisting of Ru(II)$(bpy)_2$(LL′) Complexes and [60]Fullerene (or Carbon Nanotube)

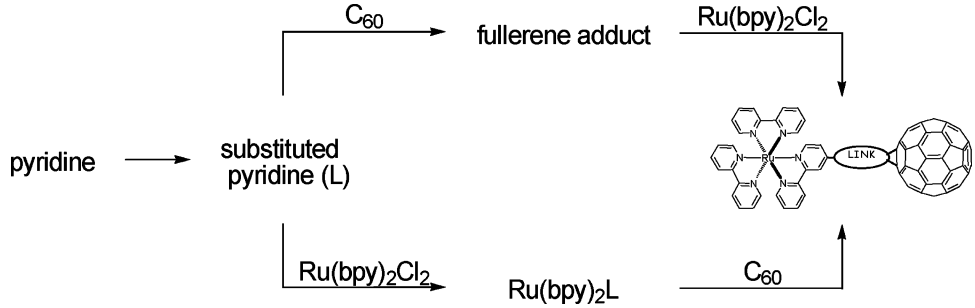

platinum microelectrode (diameter 25 μm, polished prior to measurements). The counter electrode was a platinum wire, mounted very close to the working and reference electrodes. Potentials were measured against a silver wire pseudoreference, and $FcPF_6$ was added to the electrolyte after measurements to set the pseudoreference versus $Fc^{+/0}$. All potentials reported here are given versus the $Fc^{+/0}$ couple by subtracting 0.21 V from the potentials measured versus the pseudoreference.

Steady-State Emission and Emission Quantum Yields. The emission spectra were recorded on a SPEX Fluorolog II fluorimeter equipped with double monochromators for excitation and emission. The emission upon 452 nm excitation was detected at a right angle with a R928-type PMT detector in single-photon counting mode with 3.6 or 7.2 nm resolution on the monochromators. The samples were prepared in 1 × 1 cm optical quartz cells as ca. 10 μM air-equilibrated acetonitrile solutions, with an optical density of 0.1 at 452 nm. Emission quantum yields were calculated by comparison with the emission from a sample of $Ru(bpy)_3(PF_6)_2$ in air-equilibrated acetonitrile, for which a value of $\Phi_{em} = 0.01$ was used.[32]

Femtosecond Transient Absorption. Transient absorption pump−probe measurements on the femtosecond scale were performed with a Ti:sapphire laser system, for which details on pulses and detection have been described elsewhere.[23] A fraction of the 800 nm laser output (pulse frequency 1 kHz) was converted to 1350 nm in an optical parametric amplifier (TOPAS) and tripled to 450 nm. Remaining light at 675 and 1350 nm was removed by a filter. Every second pump pulse was blocked with a 500 Hz mechanical chopper. To limit noise from shot-to-shot fluctuations of the laser, part of the pump beam was passed onto a separate photodiode whose output was used to discard pulses of too low or too high intensity. Pump energy was reduced by filters to <1 μJ (diameter <400 μm) at the sample to avoid sample degradation and nonlinear effects. The white-light probe was generated from a fraction of the 800 nm light passed through an optical delay line (<10 ns total delay) and focused onto a moving CaF_2 plate or stationary sapphire plate. The white light was split into signal and reference, of which the reference was led to the diode array detector without passing the sample. The polarization of the pump was set at magic angle (54.7°) relative to that of the probe using a polarizer and a $\lambda/2$ plate. Pump and probe were focused in a vertically moving sample cell of 1 × 10 mm, and the transmitted probe led into the detector. The reported spectra are averages of 1000−10000 individual measurements and have not been chirp corrected. A smoothing function has been applied to reduce high-frequency noise in the spectra, without distortion of the overall spectral features. Kinetic analysis was done on nonsmoothed data.

Single Wavelength Pump−Probe Measurements. The 800 nm output of the Ti:sapphire (1 kHz) setup was passed through a beam splitter into two TOPAS-White noncollinear optical parametric amplifiers whose outputs were tuned to 1010 (width > 20 nm) and 900 nm, respectively. Filters were used to remove stray wavelengths. The 900 nm light was passed through a 500 Hz mechanical chopper, a delay line with a variable optical delay (<2 ns), and then doubled in an external 0.1 mm BBO crystal to give the 450 nm pump. A $\lambda/2$ plate was used to set magic angle conditions relative to the 1010 nm probe at the sample. The combined pulse energy of pump and probe at the sample was less than 2 μJ, and the 1 mm sample cell was rotated to avoid sample degeneration. The 1010 nm light was split into probe and reference prior to the sample, and two photodiodes connected to boxcar integrators gave I and I_0, respectively. Averages of 5000−10 000 independent measurements where used.

Nanosecond Transient Absorption. Time-resolved transient absorption measurements on the microsecond time scale were performed with a frequency tripled Q-switched Nd:YAG laser (Quantel) pumping an OPO (Opotek) to obtain 450 nm, <10 ns pulse width pump light. The samples were purged with nitrogen in the 1 × 1 cm sample cell prior to measurements. Probe light was provided by a continuous wave xenon arc lamp (measurements on the microsecond time scale). The signal was detected at right angle to the incoming laser beam with a monochromator and an R928-type photomultiplier tube or a Hamamatsu Si photodiode with amplifier (for measurements at 800−1000 nm). The output was recorded on a Philips digital oscilloscope and processed with Applied Photophysics LKS60 software. When applicable, a 425 nm filter was inserted in the probe beam to avoid sample degradation from UV irradiation. The pulse energy at the sample was attenuated to <3 mJ.

Results and discussion

Synthetic Strategies. Two main routes to dyads **1**−**3** can be envisioned, each with their advantages and disadvantages. For both approaches, a main task is to find suitable solvents. Reactions involving C_{60} are preferably performed in toluene to ensure that the fullerene is completely dissolved and thus decreasing the risk of obtaining polyadducts, whereas Ru(bpy)$_n$ complexes are usually only soluble in more polar solvents.

The most common stepwise approach (upper route in Scheme 1), with construction of a ligand bearing the [60]fullerene followed by assembly of the dye, was used in our original preparation of dyads **1**−**3**.[31] Purification and recovery of nonreacted starting materials as well as thorough solution-phase NMR characterization of intermediates is feasible, but the presence of the carbon cage over several synthetic steps may decrease both stability and solubility of the isolated intermediates.

(32) Calvert, J. M.; Casper, J. V.; Binstead, R. A.; Westmoreland, T. D.; Meyer, T. J. *J. Am. Chem. Soc.* **1982**, *104*, 6620–6627.

Scheme 2. Preparation of Complexes of the Type $Ru(bpy)_2(\eta^2\text{-L})$, (**1**−**5**)[a]

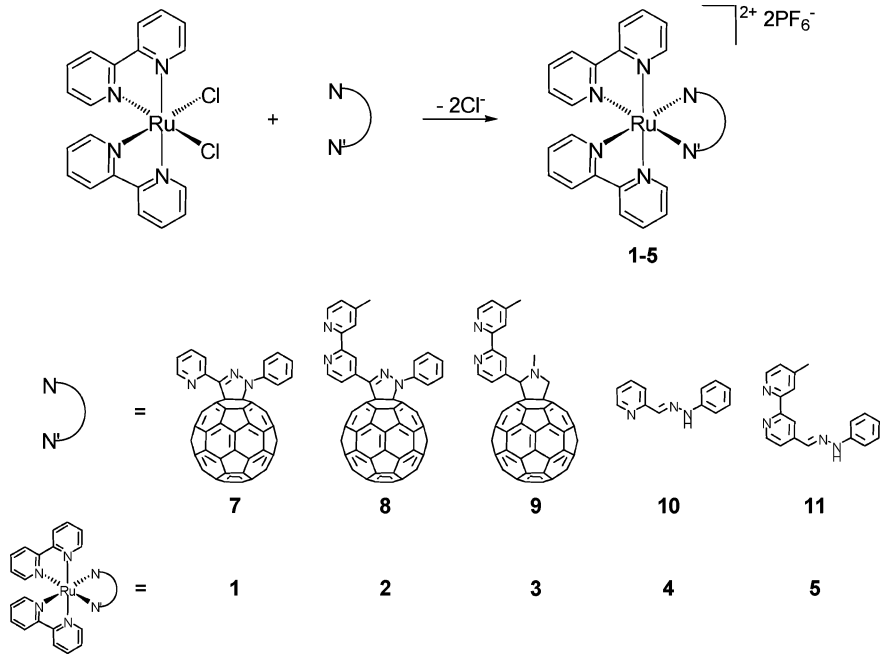

[a] The chloride ions are, in the preparation of **1** and **2**, removed by reaction with $AgBF_4$.

By connecting the cage in the last step (Scheme 1, lower route), problems concerning instability of intermediate products can be decreased. On the other hand, in our hands, the final step was only moderately efficient. For example, ^{1}H NMR signals from the pyrrolidine unit of dyad **3** was observed in the crude mixture from a reaction of $Ru(bpy)_2$(LL-4-CHO) under pyrrolidination conditions, carried out in toluene where the dye component and the products were only sparingly soluble. The solubility of the product mixture in toluene, acetone, and chloroform, and so forth was too low to achieve an efficient separation of **3** from starting materials and other reaction products. Similar observations from reactions using **5** under hydrazone formation conditions strongly indicates that this route is inferior to the stepwise approach for efficient preparation of our short-link [60]fullerene dyads. However, in cases where multiple additions of dye units to insoluble carbon materials are desired, this route would be the most practical one provided that key spectroscopical properties of the dye components are known and sufficiently different from those of the final dyad for the chemical outcome of the final step to be assessed, as is the case for precursor complexes **4** and **5**.

Formation of Dyads with Addition of $(bpy)_2$Ru(II) in the Final Step. Complexes with η^2 -coordinated ligands belonging to the $Ru(bpy)_2(LL')$ group are usually prepared by heating $Ru(bpy)_2Cl_2$ and ligand LL′ in a polar solvent such as ethanol or mixtures of ethanol and water, followed by addition of an excess of a PF_6^--containing salt. This exchange of counterions from Cl^- to PF_6^- makes the resulting complex less polar, thus making possible isolation by extractive methods or by collecting the precipitate, if formed. This approach, which worked well for the preparation of **4** and **5**, was not applicable to the preparation of **1**−**3**. As the fullerene-containing ligands **7**−**9** are significantly less polar than, for example, their nonsubstituted analogues **10** and **11**, their solubility in ethanol is too low for the desired reaction to occur. A nonpolar solvent such as toluene would, on the other hand, not dissolve $Ru(bpy)_2Cl_2$ well enough. Fortunately, the solubility of the components was sufficiently high in a 1:1 mixture of toluene and ethanol for some reaction to occur, and, upon addition of NH_4PF_6, precipitates were obtained that displayed UV−vis spectroscopic features characteristic for ruthenium bipyridine complexes, such as broad absorption bands between 400 and 500 nm.[31] Further characterization was less straightforward as only **3** was stable enough for successful purification. Therefore, other solvents and solvent combinations were tried for the formation of the least stable **1**.

The crucial step is the exchange of the two chloride ligands for the neutral LL′ ligand. In general, chloride is a strongly coordinating ligand, and its complexes are often polar, thus the introduction of highly nonpolar and/or weakly coordinating ligands might be problematic, in particular if the components are not completely soluble in the reaction solvent. We found that neither the reactions in a mixture of carbon disulphide and ethanol, nor those in THF, in which both the ruthenium salt and ligand **7** were fully soluble, resulted in any useful yield of isolable product. This was the case also for the attempts using the more high-boiling mixture of toluene and 2-methoxyethanol. An alternative one-pot stepwise approach, where the chloride ligands of $Ru(bpy)_2Cl_2$ were exchanged for the noncoordinating counterion BF_4^-, was found to be more successful, in line with established knowledge in the field of Pd(II) coordination chemistry,[33–35] but with only a few examples for bipyridine ruthenium Ru(II) complexations.[12,15,36,37]

Treatment of $Ru(bpy)_2Cl_2$ with $AgBF_4$ in the presence of ligand **7** (Scheme 2) resulted in precipitation of AgCl and **1**

Table 1. Redox Potentials and Resulting Charge State Energies of **1**−**5**

	$E_{1/2}$ $Ru^{III/II}$ [a]	$E_{1/2}$ $C_{60}^{0/-}$ [a]	E_{CS} [b] /eV
1	0.94	−0.87	1.81
2	0.86	−0.76	1.62
3	1.06	−0.67	1.73
4	0.95		
5	0.83		

[a] V vs $Fc^{+/0}$, acetonitrile, 0.1 M $TBAPF_6$, 298 K. [b] Energy of charge-separated state, calculated as $E_{CS} = e[E_{1/2}^{ox} - E_{1/2}^{red}]$; e.g. for compound **1** $E_{CS} = e[E_{1/2}(Ru(III/II)) - E_{1/2}(C_{60}^{0/-})] = e[0.94 + 0.87]$ eV = 1.81 eV.

with high purity was obtained after a workup with exchange of BF_4^- for PF_6^-, whereas use of $AgPF_6$ resulted in a nonidentified product that, unexpectedly, was soluble in water. Following the successful protocol with $AgBF_4$, **2** was obtained after a straightforward isolation process. Interestingly, both **1** and **2** from this route were significantly more stable than those from previous attempts. In particular, **1** from the silver-assisted route was, in fact, air stable in solution for hours. In contrast to the observations for the silver-assisted preparation of **1** and **2**, treatment of $Ru(bpy)_2Cl_2$ with silver salts in the presence of **9** did not lead to any significant improvement of the reaction outcome compared to the silver-free cases.

All dyads exist as isomeric mixtures, with a ruthenium-centered chiral center and a potentially stereogenic tertiary amine in the linking motif. In general, pyramidal inversion of less-hindered amines (as in **2** and **3**) is considered as being a rapid process, but the two sets of *N*-phenyl protons observed for **1** is an indication of an exceptionally hindered inversion of the amine unit in this complex. In **3**, there is an additional stereocenter at the bipyridinyl-substutited pyrrolidine carbon atom. Thus, **1** and **3** exist as at least two sets of diastereomers, whereas **2** likely is a racemate. In a nonchiral environment, the physical properties of enantiomers are identical, whereas those of diastereoisomers may differ.

Electrochemical Characterization. The half-wave potentials for the first oxidation and reduction, as determined by cyclic voltammetry and differential pulse voltammetry (Supporting Information), are presented in Table 1. All potentials are reported versus the $Fc^{+/0}$ redox couple. For all complexes, the first reversible oxidation wave appears at $E_{1/2} = 0.8-1.0$ V versus $Fc^{+/0}$, which is typical for the Ru(III/II) oxidation in ruthenium polypyridine complexes. In **1**−**3**, the first reversible reduction process is observed at $E_{1/2} = -0.6$ to 0.9 V versus $Fc^{+/0}$, and is assigned to the first reduction of the C_{60} unit. Table 1 also presents the energies of the charge separated states of **1**−**3**, calculated from the corresponding half-wave potentials. The Coulombic work tem is not included in the calculations; although not negligible it is expected to be constant throughout the series.[38]

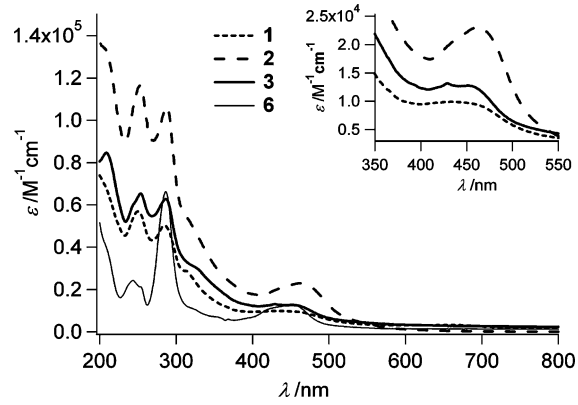

Figure 1. UV−vis absorption spectrum of **1**−**3** and the global reference **6** (air-saturated acetonitrile, 298 K).

Absorption and Emission Properties. In the visible region, the absorption of C_{60} is weak, whereas complexes belonging to the $Ru(bpy)_3$ group exhibit characteristic MLCT (metal-to-ligand charge transfer) absorption bands between 400 and 500 nm. This is observed also for **1**−**5**. In analogy with the parent compound $[Ru(bpy)_3](PF_6)_2$ (**6**), **1**−**3** show a broad MLCT absorption at 430−470 nm and a LC (ligand-centered) band at approximately 285 nm (Figure 1). **1**−**3** also show absorption features typical for 6,6-substituted fullerenes, with bands at 250 and 310 nm.[12] The spectrum of **3** displays the small but sharp peak at 430 nm characteristic for fulleropyrrolidines.[15] In addition, **1**−**3** all display weak absorption to the red of the MLCT band. This feature most likely stems from the nonzero absorption of [60]fullerene in this region. Interestingly, the absorption coefficients of both the MLCT and LC bands of **2** were found to be much higher than those of **1**, **3**, and **6** (whereas the values for **6** agree well with literature[1]). This unexpected observation was reproduced for several solutions of **2** but was not further investigated.

The ground-state absorption spectrum of **4** (Supporting Information) is fairly similar to that of **1** and **6**. By contrast, the ground-state absorption of **5** in acetonitrile is very different from that of **2** and **6**, with additional bands at about 390 and 560 nm due to the appended hydrazone. Also, large changes in ground-state absorption were observed for **5** when changing the solvent from acetonitrile to dichloromethane. This was not observed for the other complexes studied.

Absorption and emission properties of **1**−**5** indicate that the level of emitting impurities, such as $Ru(bpy)_3$, is unusually low. Only trace emission was found, which for **1**−**3** indicates an effective quenching of the ruthenium ^{3}MLCT state emission. This is consistent with the very fast energy transfer that was observed in time-resolved studies of **1**−**3** (below). Complexes very similar to **4** have been reported to show very weak emission at ambient temperature, and this behavior is sensitive to the nature of the substituents on the hydrazone ligand.[39,40] An intact non-coordinated

(33) Anderson, C. B.; Burreson, B. J. *J. Organomet. Chem.* **1967**, 7.
(34) Albinati, A.; Ammann, C. J.; Pregosin, P. S.; Rüegger, H. *Organometallics* **1990**, 9.
(35) Gogoll, A.; Johansson, C.; Axén, A.; Grennberg, H. *Chem.—Eur. J.* **2001**, 7.
(36) Lou, Y.; Potvin, P. G.; Tse, Y.-H.; Lever, A. B. P. *Inorg. Chem.* **1996**, *35*, 5445–5452.
(37) Hammarström, L.; Norrby, T.; Stenhagen, G.; Mårtensson, J.; Åkermark, B.; Almgren, M. *J. Phys. Chem. B* **1997**, *101*, 7494–7504.

(38) The Coloumbic work tem is estimated to approximately 0.1 eV, within the crudness of the hard sphere-continous medium model.

(39) Bolger, J. A.; Ferguson, G.; James, J. P.; Long, C.; McArdle, P.; Vos, J. G. *J. Chem. Soc., Dalton Trans.* **1993**, *1993*, 1577–1583.
(40) Abrahamsson, M.; Hammarström, L.; Tocher, D. A.; Nag, S.; Datta, D. *Inorg. Chem.* **2006**, *45*, 9580–9586.

Table 2. Absorption and Emission Properties of **1**−**3**[a]

	MLCT absorption	Emission	
	λ_{max}/nm (ϵ /M^{-1} cm^{-1})	λ_{max}/nm	Φ_{em}
1	435 (9900)	620	1×10^{-4}
2	461 (23 000)	625	2×10^{-4}
3	451 (13 000)		$\ll 1 \times 10^{-4}$
4	440 (n.d.)		$\ll 1 \times 10^{-4}$
5	463 (n.d.)[b]	640	8×10^{-4}
6[c]	452 (13 000)	615	1×10^{-2}[d]

[a] All measurements were performed in air-saturated acetonitrile at 298 K. [b] additional bands at 366 and 550 nm that might have some MLCT character [c] Values from ref 1. [d] Based on values from ref 32.[41]

hydrazone unit influences the wavelength of maximum emission, as seen for **5**, which is significantly different from that of both **2** and **6**. Thus, the [60]fullerene unit has a substantial influence on the intrinsic photophysical properties of **1**−**3**, and despite the similarities in the first coordination sphere to **4** and **5**, the intrinsic photophysics are remarkably different. Therefore, both **4** and **5** could, in principle, be used as dye components in dyadization of carbon materials, as discussed above, since neither of them exhibit identical photophysical properties as do **1** and **2**, respectively (Table 2).

Time-Resolved Spectroscopy. Femtosecond transient spectra of **1**−**3** at representative times after excitation at 450 nm are shown in Figure 2. The compounds exhibit very similar general behavior. Immediately after excitation, a bleach of the MLCT ground-state absorption is seen at 450−500 nm, as well as the unstructured absorption at $\lambda >$ 500 nm expected for the ruthenium polypyridyl ^{3}MLCT state. In **1**, the bleach is less pronounced. At 1 ps after excitation, a broad absorption with a maximum at 690 nm has formed. This is where the fullerene triplet excited state $^3C_{60}$* is expected to give a positive absorption. Simultaneously, the MLCT ground-state has recovered, which suggests reformation of a Ru(II) species.

A global fit of the data at five wavelengths covering the observed spectral range shows that three time constants are necessary to describe the kinetics (Table 3). The growth of the $^3C_{60}$* absorption and simultaneous recovery of the MLCT ground-state absorption is very fast (τ_1 and a minor component τ_2). The final spectrum decays with a component ($\tau_3 \gg$ 10 ns) that is slower than can be resolved in our femtosecond experiments. Upon nanosecond excitation, the initial excited spectra of **1**, **2**, and **3** correspond to the respective final spectrum in the femtosecond measurements (Supporting Information). These spectra decay with time constants in the microsecond range. The long lifetime and spectral features agree well with previous reports on the fullerene $^3C_{60}$* state.[12]

Because the expected energy of the charge separated state (1.6−1.8 eV, Table 1) is lower than that of the first excited ^{3}MLCT state (2.1 eV in Ru(bpy)$_3$), a thermodynamically feasible route to the fullerene T_1 state (1.5 eV in pristine C_{60}) would be through a charge separated (CS) state, as shown in Scheme 3. If this charge separated state were

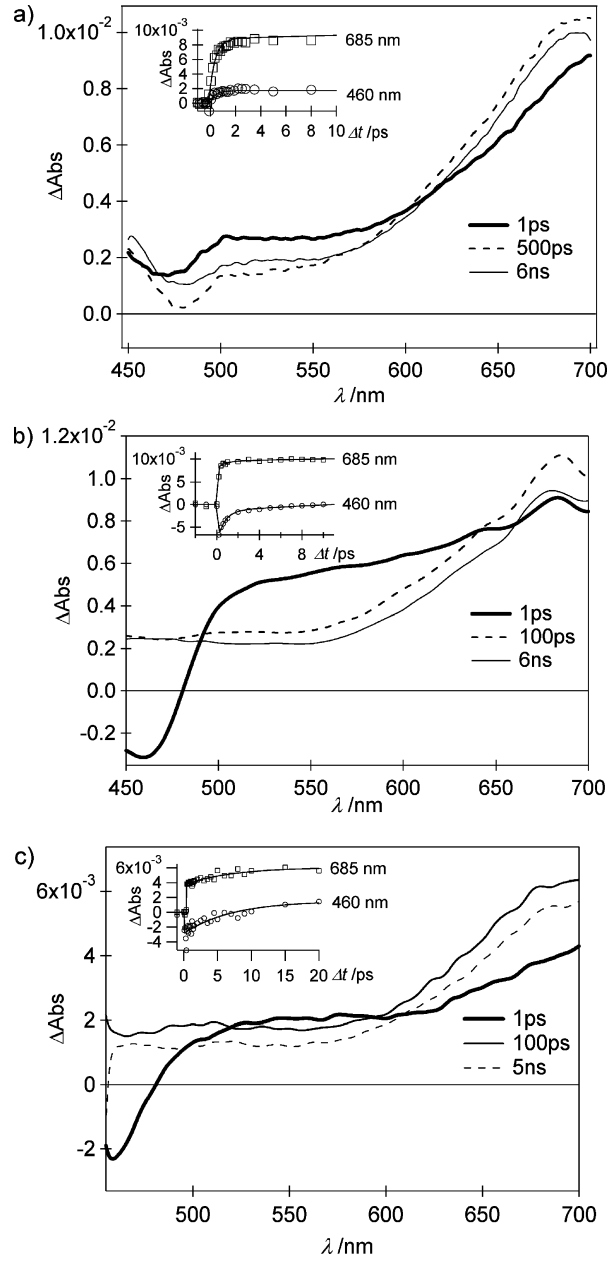

Figure 2. Transient absorption of **1** (a), **2** (b), and **3** (c) upon 450nm excitation (air-saturated acetonitrile, 289 K). The insets show the dynamics at early delay times at 460 nm (circles) and 685 nm (squares).

Table 3. Time Constants of Transient Absorption Rise (τ_1, τ_2) and Decay (τ_3) for **1**−**3** in Acetonitrile, 298 K

	τ_1 /ps [a]	τ_2 /ps [a]	τ_3 /μs[b]
1	0.5	23 (7%)[c]	28
2	0.7	25 (11%)[c]	1.3
3	7	250 (3%)[c]	42

[a] Air-saturated solvent. [b] Deaerated solvent. [c] Percentage of the $^3C_{60}$* absorption rise.

populated, features from the fullerene radical would be observed in the spectra. The fullerene radical anion $C_{60}^{\bullet -}$ is reported to have a broad, moderately strong absorption around 1000 nm (for fulleropyrrolidines $\epsilon_{\lambda\ =\ 1010nm} = 8000$ M^{-1} cm^{-1}).[12] Although this band shifts with functionalization, it should, if present, dominate over the absorption of the ruthenium moiety in the near-IR region (for Ru(bpy)$_3$,

(41) A value of 0.01 is used for Ru(bpy)$_3$ in air-equilibrated acetonitrile. This is based on the Ru(bpy)$_3$ emission lifetime with and without air and an emission quantum yield of 0.6 in deairated acetonitrile, from ref 33.

Scheme 3. Approximate Energy Levels of the Relevant Excited States and Charge Separated States of **1**−**3**[a]

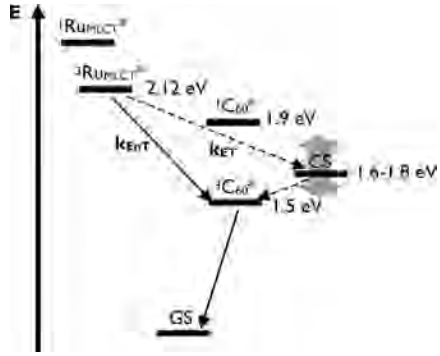

[a] Energies for the $^3Ru_{MLCT}$, $^1C_{60}$*, and $^3C_{60}$* states were taken from **6** and pristine C_{60}; the energies for the CS states were taken from Table 1. Solid arrows indicate the observed processes.

$\epsilon_{\lambda = 1000nm} \approx 1500\ M^{-1}\ cm^{-1}$).[42] However, single-wavelength pump−probe measurements on **1**, **2**, and **3** at 1010 nm did not show any growing signal, and the observed kinetics match those in the visible region of respective compound well. Thus, evidence for electron transfer is lacking.

Further support for rapid energy transfer as the dominant quenching pathway comes from the observation that changing solvent from acetonitrile to dichloromethane does not at all produce as dramatic an effect on the Ru(II) excited-state deactivation rates as one would expect if an intermediate charge-separated state was involved. Qualitatively, the spectral evolution on the femtosecond time scale is the same in dichloromethane as in acetonitrile. Again, three kinetic components are needed for a satisfactory global fit to the data; a fast component $\tau_1 = 0.5$, 0.4, and 2.5 ps (for **1**, **2**, and **3**, respectively), a minor component $\tau_2 = 150$, 70, and 30 ps (**1**, **2**, and **3**) and for the decay of the final spectrum $\tau_3 > 10$ ns (for **3** in dichloromethane, $\tau_3 = 3.8$ ns). Compared to acetonitrile, the solubility of **1**−**3** is significantly poorer in dichloromethane.

We have considered some possible explanations for the intermediate component τ_2, which represents only a small fraction of the overall process. τ_2 shows a marked solvent dependence, in contrast to the τ_1 component, something that could indicate that aggregates are involved. However, we assume that we have only monomeric units in acetonitrile. Other possible explanations, such as different photophysical properties for the diastereomers (vide supra), intersystem crossing, interligand hopping, or electron transfer from a nonthermalized ^{3}MLCT state,[43–45] are unlikely on the basis of the range of lifetimes, the observed solvent dependence, and considering the small amplitude of the τ_2 component. We cannot exclude a small amount of impurity, possibly due to photodegradation during measurements.

In all, the observations suggest a mechanism in which the ^{3}MLCT states of **1**−**3** are quenched by rapid energy transfer from the ruthenium moiety to the fullerene, resulting in rapid population of the fullerene T_1 excited state. Most likely, the dominating mechanism for energy transfer is electron exchange, since donor and acceptor are close enough for significant orbital overlap and the Förster spectral overlap is small. The energy transfer is very fast ($k_{obs} > 1.4 \times 10^{11}$ s^{-1}) for the fulleropyrrolidino **3** and even faster ($k_{obs} > 1 \times 10^{12}$ s^{-1}) in the fulleropyrazoline **1** and **2** (acetonitrile, 298 K). The different rates might be explained by the slight increase in donor−acceptor distance in **3** compared to that in **1** and **2**, since there is an exponential decrease of the coupling matrix element with donor−acceptor distance in electron exchange energy transfer. Furthermore, the nonconjugated bridging ligand in **3** should result in a decreased orbital overlap. However, all energy transfer rates are significantly faster than previously reported energy transfer rates in $Ru(bpy)_3$-C_{60} dyads.[21–24] The extremely fast energy transfer suggests a fullerene triplet quantum yield close to unity. This is confirmed by the magnitude of transient absorption changes, which are in agreement with quantitative $^3C_{60}$* triplet formation, given the uncertainty in relative extinction coefficients (Supporting Information).

Conclusions

We have shown that formation of heteroleptic complexes from $Ru(II)(bpy)_2Cl_2$ and bidentate ligands LL′ can be facilitated if the reactions are carried out in the presence of an Ag(I) salt, both in formation of complexes of the tris-bipyridine type and in efficient ligation of a pyrazole−pyridine ligand. Exchanging the strongly coordinating chloride ions for more weakly bound counterions facilitates the coordination of the neutral ligand, thus allowing the resulting complex to form at lower temperatures and in less-coordinating solvents. For the pyrazoline-linked dyads **1** and **2**, the products from the silver-assisted route were of higher purity than what have been obtained previously, and the stability of the complexes was sufficient for spectroscopic characterization. Both absorption and emission data indicate that the studied complexes have unusually low levels of emitting impurities. We attribute this to the mild conditions, where exchange of organic ligands can be kept at a minimum.

The observed rate of energy transfer is significantly faster than for comparable dyads previously reported in the literature. This can be explained by the short donor−acceptor distance and in particular by the strong coupling afforded by the pyrazoline link of **1** and **2**. This provides a means of efficient sensitization of the [60]fullerene to visible light in the 300−500 nm region. Despite the close proximity of donor and acceptor in dyads **1**−**3**, electron transfer is not fast enough to successfully compete with the energy transfer, neither for pyrrolidine-linked nor for pyrazoline-linked dyads. It will not be sufficient to manipulate the distance nor the redox properties of the [60]fullerene by the pyrazoline functionalization (as in **1** and **2**) to obtain a long-lived charge separated state in this type of dyads. An alternative strategy, and the only realistic one in the case of modifications of carbon materials with Ru-polypyridyl

(42) Shimizu, O.; Watanabe, J.; Naito, S. *Chem. Phys. Lett.* **2000**, *332*, 295–298.
(43) Yeh, A. T.; Shank, C. V.; McCusker, J. K. *Science* **2000**, *289*, 935–938.
(44) Damrauer, N. H.; Cerullo, G.; Yeh, A.; Boussie, T. R.; Shank, C. V.; McCusker, J. K. *Science* **1997**, *275*, 54–57.
(45) Wallin, S.; Davidsson, J.; Modin, J.; Hammarström, L. *J. Phys. Chem. A* **2005**, *109*, 4697–4704.

donors, is to improve the donor properties of the $Ru(bpy)_n$ moiety by the use of other ligand systems.

Acknowledgment. This work was supported by the Swedish Foundation for Strategic research (CARAMEL), the Swedish Research Council, the Göran Gustafsson Foundation, the Swedish Energy Agency and the Knut and Alice Wallenberg Foundation. We thank Mr. Henrik Johansson and Mr. Aurélien Journée for assistance in the preparation of **3** and Dr. George Tsekouras for his kind help with the small-volume electrochemical characterization.

Supporting Information Available: Experimental details for the alternative route to **3**. Electronic absorption spectra of **4** and **5** in acetonitrile and dichloromethane, electronic absorption spectra of **1**−**3** in dichloromethane and transient absorption upon nanosecond excitation of **1**−**3** in deaerated acetonitrile. Fullerene triplet yields for **1**−**3**, estimated from transient absorption data. Small-volume cyclic voltammetry for **1**−**5** in acetonitrile ($TBAPF_6$ electrolyte). ^1H NMR (TOCSY) of **1**, **2**, **4**, and **5**. This material is available free of charge via the Internet at http://pubs.acs.org.

IC800168D